JOURNAL OF VIROLOGY, Oct. 2008, p. 9445–9457 Vol. 82, No. 19
0022-538X/08/$08.00+0 doi:10.1128/JVI.00835-08

Human Immunodeficiency Virus Type 1 Envelope gp120 Induces a Stop Signal and Virological Synapse Formation in Noninfected CD4$^+$ T Cells$^{\nabla}$†

Gaia Vasiliver-Shamis,[1] Michael Tuen,[2] Teresa W. Wu,[1] Toby Starr,[1] Thomas O. Cameron,[1] Russell Thomson,[1] Gurvinder Kaur,[2,3] Jianping Liu,[2] Maria Luisa Visciano,[2] Hualin Li,[2] Rajnish Kumar,[2] Rais Ansari,[4] Dong P. Han,[4] Michael W. Cho,[4] Michael L. Dustin,[1] and Catarina E. Hioe[2]*

Program in Molecular Pathogenesis, Marty and Helen Kimmel Center for Biology and Medicine, Skirball Institute for Biomolecular Medicine, New York University School of Medicine, New York, New York 10016[1]; Veteran Affairs New York Harbor Healthcare System, Manhattan Campus, and Department of Pathology, New York University School of Medicine, New York, New York 10010[2]; Department of Transplant Immunology and Immunogenetics, All India Institute of Medical Sciences, Ansari Nagar, New Delhi, India[3]; and Department of Medicine, Case Western Reserve University School of Medicine, Cleveland, Ohio 44106[4]

Received 18 April 2008/Accepted 9 July 2008

Human immunodeficiency virus type 1 (HIV-1)-infected T cells form a virological synapse with noninfected CD4$^+$ T cells in order to efficiently transfer HIV-1 virions from cell to cell. The virological synapse is a specialized cellular junction that is similar in some respects to the immunological synapse involved in T-cell activation and effector functions mediated by the T-cell antigen receptor. The immunological synapse stops T-cell migration to allow a sustained interaction between T-cells and antigen-presenting cells. Here, we have asked whether HIV-1 envelope gp120 presented on a surface to mimic an HIV-1-infected cell also delivers a stop signal and if this is sufficient to induce a virological synapse. We demonstrate that HIV-1 gp120-presenting surfaces arrested the migration of primary activated CD4 T cells that occurs spontaneously in the presence of ICAM-1 and induced the formation of a virological synapse, which was characterized by segregated supramolecular structures with a central cluster of envelope surrounded by a ring of ICAM-1. The virological synapse was formed transiently, with the initiation of migration within 30 min. Thus, HIV-1 gp120-presenting surfaces induce a transient stop signal and supramolecular segregation in noninfected CD4$^+$ T cells.

Human immunodeficiency virus type 1 (HIV-1) infection occurs most efficiently by direct virus transfer from infected cells to uninfected target cells (12, 44, 53), but the mechanisms for such cell-to-cell transfer are still unclear. One predominant mode of HIV-1 transfer between CD4$^+$ T cells has been shown to involve a virological synapse (VS), which is an actin-dependent cell-cell junction formed upon the engagement of HIV-1 envelope gp120, on the infected cell, with its receptors CD4 and the chemokine receptor (CKR) CCR5 or CXCR4 on the target cell (8, 35, 37). Notably, the HIV-1 VS is also enriched with other cellular proteins such as LFA-1 and its ligands ICAM-1 and ICAM-3, tetraspanins, and lipid raft marker GM-1 (35, 36, 38). LFA-1 in particular is recruited to the VS interface mainly on the target cell side, and the interaction with its ligands ICAM-1 and ICAM-3 on the opposing infected cell facilitates VS formation and, subsequently, HIV-1 transfer (36). The importance of the LFA-1–ICAM-1 interaction in HIV-1 infection has also been documented in other experimental systems. ICAM-1 expression was shown to be upregulated in HIV-1-infected T cells and lymphoid tissues (19, 21), and the higher levels of ICAM-1 molecules incorporated into the membrane of the budding virus particles correlated with enhanced virus infectivity (52, 65). LFA-1 expression on target cells promoted the initial processes of HIV-1 infection as well as subsequent replication and cell-to-cell transmission (23, 27, 64). Additionally, the regulation of LFA-1 activity through cytoskeleton remodeling and signaling components like phospholipase Cγ and zeta-associated protein 70 (ZAP70) was reported to modulate the efficiency of HIV-1 entry into activated target T cells (66). ZAP70 was also required for the efficient cell-to-cell transmission of the virus (58). Nevertheless, little is known about how the viral proteins and the cellular adhesion molecules are actually assembled and organized in VS.

It has been postulated that the VS resembles the immunological synapse (IS) in its molecular organization (35). The IS is a specialized cell-cell contact between a T cell and an antigen-presenting cell that is formed following T-cell receptor (TCR) recognition of the cognate peptide-major histocompatibility complex (pMHC) (17, 18). The IS is organized into distinct areas known as the supramolecular activation complexes (SMAC); in a mature IS, TCR/pMHC and protein kinase Cθ cluster at the central SMAC (cSMAC) and are surrounded by a ring of LFA-1–ICAM-1 interactions and talin known as the peripheral SMAC (pSMAC) (22, 48). Similar supramolecular organizations were implied for both the human T-cell lymphotropic virus type 1 VS (29) and HIV-1 VS (39) but, due to low-resolution microscopy, were never clearly

* Corresponding author. Mailing address: VA Medical Center, 423 E. 23rd St., Room 18-124 North, New York, NY 10010. Phone: (212) 263-6769. Fax: (212) 951-6321. E-mail: catarina.hioe@med.nyu.edu.

† Supplemental material for this article may be found at http://jvi.asm.org/.

$^{\nabla}$ Published ahead of print on 16 July 2008.

demonstrated. Importantly, the TCR engagement in the IS delivers stop signals to naturally motile T cells such that an antigen-specific interaction can be established between the T cells and antigen-presenting cells, and the ring of adhesion molecules, in particular, is essential for stopping locomotion while maintaining the structural elements of a motile cell like a highly sensitive lamellipodium (13, 14, 49, 56). Moreover, the IS allows the directional transfer of signals or molecules between two distinct cells in the absence of cell-cell fusion (15). Since cell-to-cell transmission of HIV-1 is facilitated by direct cell-cell contact that must be maintained at least for the duration of virus transfer, we hypothesize that the HIV-1 envelope, upon binding to its receptors, may deliver stop signals that arrest T-cell motility and induce the assembly of a VS with IS-like supramolecular structures.

In this study, we assessed the capacity of a surface-presented HIV-1 envelope to arrest the spontaneous motility of primary activated $CD4^+$ T cells using a transmigration assay. Subsequently, we utilized the planar bilayer system that has been valuable for studies of IS to determine the molecular organization of the VS and monitor the dynamics of VS assembly and disassembly in real time. The results demonstrate that, indeed, the interaction of HIV-1 envelope gp120 with CD4 transiently stopped $CD4^+$ T cells from migrating on ICAM-1 and induced VS formation. The data also revealed for the first time an en face view of the VS, where the HIV-1 envelope clustered in the center, forming a cSMAC-like structure, and segregated from ICAM-1 that accumulated in a pSMAC-like structure. Such transient VS formation may be critical for three functions relevant to HIV-1 spread: HIV-1 transfer from infected cells to target $CD4^+$ cells, the prevention of HIV-1 envelope-mediated cell-cell fusion, and the migration of newly infected cells to the surrounding tissues.

MATERIALS AND METHODS

Cells. Peripheral blood mononuclear cells from healthy donors were isolated from leukopacks (New York Blood Center) using Ficoll-Paque Plus (Amersham Biosciences, NJ). The New York University Institutional Review Board has reviewed the use of human specimens for this study. Samples were depleted of adherent cells by plastic adherence in complete medium (RPMI 1640 medium supplemented with 10% fetal calf serum, 2 mM L-glutamine, 100 U/ml penicillin, and 100 μg/ml streptomycin) for 1 h at 37°C. Nonadherent cells were collected, and naïve $CD4^+$ T cells were enriched using a negative-selection magnetic bead kit (Miltenyi Biotech, CA). The cell composition (>85% naïve $CD4^+$ cells) was confirmed by flow cytometry. The naïve $CD4^+$ T cells were then activated on plates coated with anti-CD3 and anti-CD28 antibodies at 5 μg/ml each (BD Pharmingen, CA). After 48 h, the cells were transferred onto new plates at a density of 1×10^6 cells/ml and supplemented with 100 U/ml interleukin-2 (NIH). Activated cells were used for transmigration assays and bilayer experiments 6 to 12 days after activation.

Transmigration assay. The assay was performed using a protocol described previously by Bromley et al. (5), with some modifications. The filters of transwell inserts with a 5-μm pore size (Corning, MA) were coated with sheep antibodies to the C terminus of gp120 (10 μg/ml) to capture gp120 or HIV-1 virions in the presence or absence of ICAM-1. Aldrithiol-2-inactivated HIV-1 IIIB virions grown in CEMx174(T1) cells were a gift of Jeffrey Lifson (SAIC Frederick, NCI). Recombinant soluble $gp120_{JRFL}$ was provided by the NIH NIAID Division of AIDS Vaccine Research Program through Jon Warren. Recombinant $gp120_{BH10}$ and $gp120_{D368R}$ were produced in our laboratory from transfected CHO cells. The gp120 proteins were used at a fixed amount of 10 μg/ml or diluted 10-fold starting from 10 μg/ml to attain the densities of 120 to 0 molecules/μm^2. For comparison, antibodies to CD3 (OKT3), CD4 (OKT4 and RPA-T4), CD43 (290111), or CD58 (248310) were also tested in the presence of ICAM-1. The activated $CD4^+$ T cells were then added to the top wells while medium was added to the bottom wells. In some experiments, SDF-1α (R&D Systems, MN) was added to the bottom wells. When the cells or the filters were treated with antibodies or CKR antagonists, these reagents were kept throughout the assays. After incubation for the designated time periods, the cells transmigrating to the bottom wells were counted by a flow cytometer using known concentrations of small latex beads (Invitrogen, CA) as an internal standard.

Visualization of virological synapse using the planar bilayers. Mouse ICAM-1 with a glycosylphosphatidylinositol (GPI) anchor was labeled with Cy5 (Cy5–ICAM-1–GPI) and incorporated into liposomes as described previously (17, 22). It was previously shown that human LFA-1 binds to mouse ICAM-1 (34). The ICAM-1 density was adjusted with dioleoylphosphatidylcholine liposomes and used in the bilayers at 200 to 250 mol/μm^2, which is similar to the density on activated T cells. To attach His_6-tagged gp120 to the bilayers, Ni^{2+}-chelating DOGS-NTA {1,2-dioleoyl-*sn*-glycero-3-[*N*(5-amino-1-carboxypentyl)iminodiacetic acid]succinyl} (Avanti Polar Lipids, AL) was included in bilayers. Bilayers were prepared by applying the liposomes onto a glass coverslip of a parallel plate flow cell (Bioptechs, Butler PA) and treated with 5% casein containing 100 μM $NiCl_2$. His_6 gp120 produced from recombinant vaccinia virus (9) was labeled with Alexa Fluor 488 (Invitrogen, CA), incubated with the Ni^{2+}-chelating bilayer for 30 min, and washed with HEPES-buffered saline containing 1% human serum albumin. For anti-CD3-containing bilayers, liposomes that contained biotin-CAP (Avanti Polar Lipids) at 2 mol% were mixed with liposomes containing Cy5–ICAM-1–GPI to prepare bilayers with 0.01 mol% biotin. Streptavidin (4 μg/ml) and Alexa Fluor 546-labeled monobiotinylated anti-CD3ε monoclonal antibody (5 μg/ml) were reacted sequentially with the biotinylated lipid bilayers. Anti-CD4-containing bilayers were prepared using monobiotinylated anti-CD4 monoclonal antibody OKT4 as described above for anti-CD3 bilayers using 0.1 mol% biotin.

The flow cell containing the bilayers was warmed up to 37°C, cells were injected in 500 μl of HEPES-buffered saline containing 1% human serum albumin, and images were collected for 1 h on a wide-field fluorescence microscope. The density of Alexa Fluor 488-gp120 molecules on the bilayer was determined by coating the same bilayer preparations onto 5-μm silica beads and analyzing the beads by flow cytometry using fluorescein calibration beads (Bangs Laboratories Inc., IN).

To assess the molecular interactions required for VS formation, the bilayers were first treated for 30 min with 20 μg/ml of each of the following anti-gp120 monoclonal antibodies: EH21, 2219, and 654 (courtesy of James Robinson, Tulane University, New Orleans, and Suzan Zolla-Pazner, New York University, New York). The cells were also suspended in buffer containing 20 μg/ml of the respective antibodies before injection to the bilayer. In some experiments, AMD-3100 and TAK-779 were used to treat the cells. These CKR antagonists were added to the cells for 30 min prior to injection to the bilayer and kept throughout the experiment.

Microscopy. Multicolor fluorescence microscopy and interference reflection microscopy (33) was performed on an automated microscope with an Olympus TIRFM module (55) and a Orca-ER cooled charge-coupled-device camera (Hamamatsu). The hardware on the microscope was controlled using Scanalytics IP-Lab software (Rockville, MD) on a PowerMac G4 Macintosh computer or Dell PC. Solamere Technology (Salt Lake City, UT) provided integration support.

Image analysis. Image processing and bilayer calibration was performed with IP-Lab and Metamorph software. Cell velocity was measured using Improvision Volocity software (Waltham, MA). A total of 150 to 1,000 cells were analyzed for each condition in all experiments presented.

Statistics. One-way analysis of variance and Dunn's multiple comparison test were done using the GraphPad Prism software (San Diego, CA).

RESULTS

HIV-1 gp120 arrests $CD4^+$ T-cell migration. To assess the effect of HIV-1 envelope on $CD4^+$ T-cell migration, we employed an assay similar to the "stop signal" experiments performed on antigen-specific T cells with agonist pMHC complexes and ICAM-1 coadsorbed to filters (5). These experiments take advantage of the rapid spontaneous transmigration of activated T cells across filters coated with ICAM-1, which separate an upper compartment, into which cells are placed initially, and a lower compartment, from which transmigrated cells are recovered. Primary human $CD4^+$ T cells that were activated with anti-CD3 and anti-CD28 monoclonal antibodies (MAbs) and cultured with interleukin-2 were used throughout the study. TCR ligands coad-

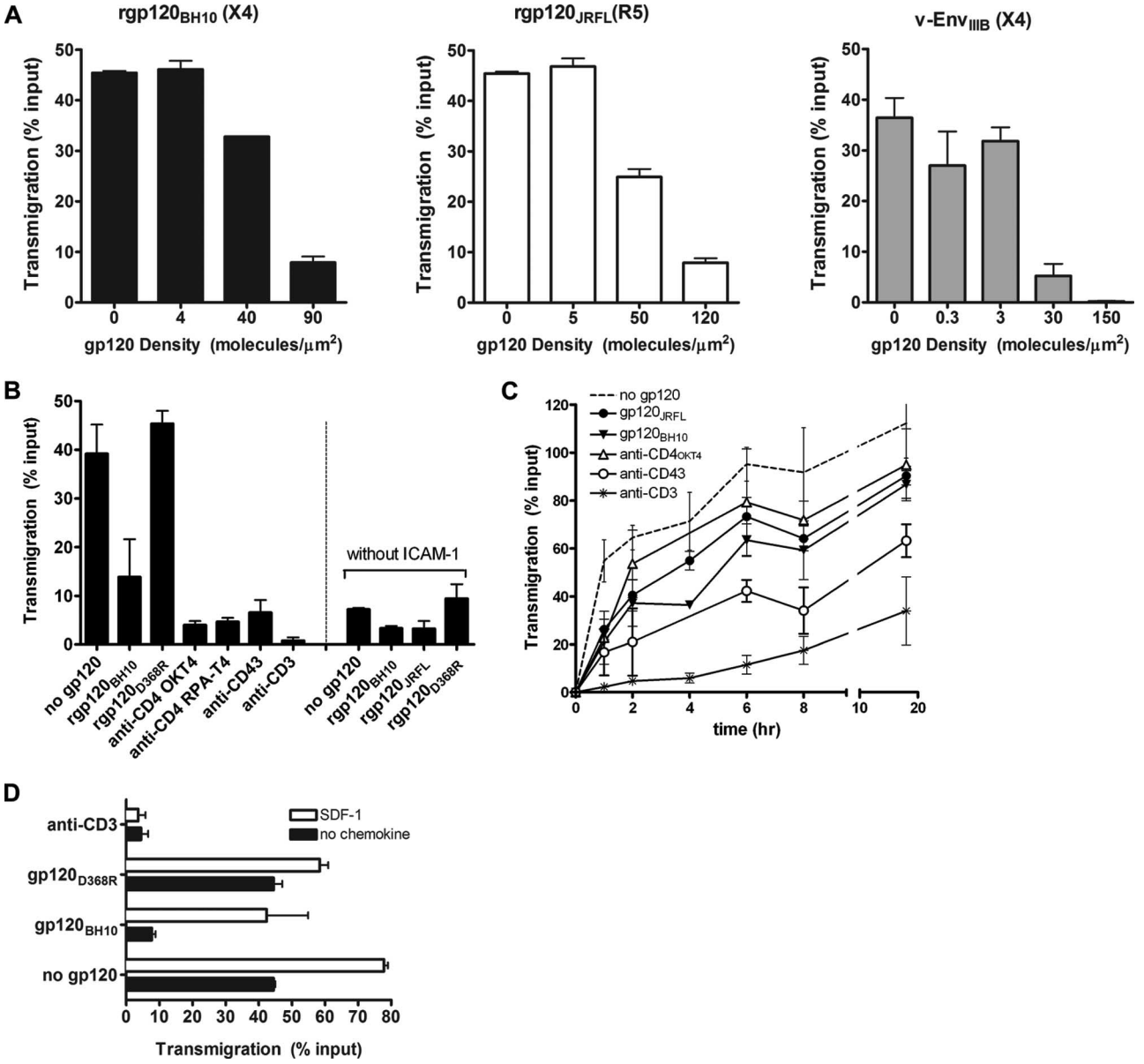

FIG. 1. HIV-1 envelope gp120 stops the spontaneous migration of human $CD4^+$ T cells. (A) Transmigration of activated human $CD4^+$ T cells was assessed through transwell filters bearing a constant amount of ICAM-1 (~200 molecules/μm^2) and different densities of recombinant gp120 (BH10 or JRFL) or native viral envelope (IIIB). The relative numbers of cells transmigrating through the filters were measured 1 h after the $CD4^+$ T cells (1×10^5 cells/well) were placed in the upper wells. (B) Transmigration of activated $CD4^+$ T cells through transwell filters coated with no gp120, $gp120_{BH10}$, $gp120_{D368R}$ that does not bind CD4, or MAbs to CD4, CD58, CD43, or CD3 in the presence of ICAM-1 or through filters coated with $gp120_{BH10}$, $gp120_{JRFL}$, $gp120_{D368R}$, or no gp120 in the absence of ICAM-1. (C) The relative numbers of $CD4^+$ T cells transmigrating through filters coated with gp120 (BH10 or JRFL), anti-CD4, anti-CD43, or anti-CD3 in the presence of ICAM-1 were compared over time from 0 to 18 h. (D) Effect of SDF-1α gradient on $CD4^+$ T-cell transmigration arrest induced by gp120 versus anti-CD3 MAb. SDF-1α (at 0 or 0.5 μg/ml) was placed into the bottom wells, while the $CD4^+$ T cells were added to the top wells. The percentages of cells migrating to the bottom wells through the filters coated with no gp120, gp120, or anti-CD3 MAb were measured after 1 h of incubation. Data from one of two or more independent experiments are shown.

sorbed with ICAM-1 to the filter stop the T cells from transmigrating by forming a synapse-like interaction characterized by a cytoskeletal polarization and a central anchoring zone (14).

In order to adapt the HIV-1 envelope into this system, we first adsorbed an affinity-purified polyclonal antibody to the C terminus of gp120 (α-gp120C) along with ICAM-1 onto a filter. α-gp120C did not reduce the transmigration of activated T cells (data not shown), which was in the range of 30 to 50% in different experiments. We then used this antibody to capture monomeric gp120 or virus-associated native envelope (Env_{IIIB}). When X4-tropic (BH10) or R5-tropic (JRFL) gp120 proteins or virus-associated native envelope (Env_{IIIB}) was captured by α-gp120C onto the filter, T-cell migration was reduced in a gp120 density-dependent manner (Fig. 1A). The virus enve-

lope appeared to be more effective, most likely due to its trimeric nature and further clustering on the viral particle. Viral particles providing an average density of 30 molecules/μm^2 were sufficient to reduce transmigration to 5%, while it requires as much as 90 to 120 molecules/μm^2 of recombinant gp120 monomers to reduce transmigration to 8%. In contrast, the D368R gp120 mutant that does not bind CD4 did not stop T-cell migration (Fig. 1B), indicating the importance of the gp120 interaction with CD4 in stopping the migration. The presence of ICAM-1 was also critical for T-cell migration; as demonstrated previously (5), very few cells transmigrated through filters containing no ICAM-1 (Fig. 1B).

For comparison, we evaluated T-cell migration through filters coated with ICAM-1 and anti-CD3 MAb, which is known to effectively deliver stop signals to migrating T cells. Indeed, ICAM-1 and anti-CD3-coated filters stopped 100% T cells at 1 h of incubation (Fig. 1B), and the CD3-mediated arrest was sustained for 18 h (Fig. 1C). In contrast, ICAM-1- and gp120-coated filters stopped 70 to 90% of the $CD4^+$ T cells at 1 h, and most cells resumed migration by 18 h (Fig. 1C). Similar results were obtained with anti-CD4 MAbs (Fig. 1B and C). This arrest pattern was distinct from that of anti-CD43 MAb, which partially retarded the cell migration throughout 18 h. CD43 has been shown to drive T-cell adhesion but is excluded from the entire CD3-mediated contact zone (6, 50) The control anti-CD58 (LFA-3) MAb that does not bind T cells caused no migration arrest. These data suggest that CD4 engagement by surface-bound HIV-1 gp120 or antibodies induces a unique pattern of T-cell migration arrest. Moreover, unlike the CD3-mediated stop signals that are insensitive to SDF-1α chemotactic activity, the presence of an SDF-1α chemokine gradient generated by adding the chemokine in the lower chamber of the transwells efficiently reversed the X4-tropic gp120-mediated arrest of T-cell migration (Fig. 1D). One possible explanation for this is that the gp120-induced stopping of T-cell migration requires gp120 binding to CXCR4, and this interaction is disrupted by SDF-1α. Alternatively, gp120 may not engage CXCR4 when stopping the T-cell migration, enabling SDF-1α to bind CXCR4 and act as a chemoattractant. Both scenarios consistently indicate distinct features of stop signals induced by gp120 versus anti-CD3 MAb. Hence, while the migratory signals induced through the CXCR4 receptor by SDF-1α have no effect on TCR stop signals, the SDF-1α migratory signals readily override and disrupt gp120-induced CD4 T-cell arrest.

To evaluate the molecular interactions involved in the gp120-induced arrest of $CD4^+$ T-cell migration, we tested soluble CD4 and human MAbs directed to different regions of gp120 for the capacity to reverse the stopping effect mediated by $gp120_{JFRL}$ and Env_{IIIB}. The addition of soluble CD4 or MAb to the CD4-binding site (CD4bs) of gp120 (654), which prevents the gp120-CD4 interaction, restored T-cell migration, while MAbs to other gp120 regions did not (i.e., anti-C1 MAb EH21, anti-V3 MAb 447, and anti-CD4-induced epitope [CD4i] MAb E51), similar to the irrelevant MAb control (anti-p24 91-5) (Fig. 2A). Anti-V3 and anti-CD4i MAbs do not block the gp120-CD4 interaction but interfere with the gp120 interaction with the CKRs CCR5 and CXCR4 (72). Anti-C1 MAb has no effect on gp120 binding to CD4 or the CKRs (25, 68). The anti-CD4 MAb that blocks CD4 binding to gp120 also reversed the stopping effect, while a nonblocking anti-CD4 MAb caused no reversal (Fig. 2B). Consistent with the data observed with anti-V3 and anti-CD4i MAbs, MAbs to the CKRs CCR5 or CXCR4 did not affect T-cell arrest induced by the corresponding R5-tropic or X4-tropic gp120 (Fig. 2B). Similarly, the addition of CKR antagonist TAK779 or AMD3100 at 10 μM, a concentration that completely blocks HIV-1 infectivity (41, 54), did not reverse the gp120-mediated arrest (Fig. 2C), indicating that the stopping of migration does not require a gp120 interaction with the CKRs. Thus, these results demonstrate that recombinant and virus-associated gp120 stops the migration of activated human $CD4^+$ T cells and that the stopping is triggered by gp120 interaction with CD4.

Reconstitution of mobile planar bilayers with HIV-1 envelope gp120. Next, we evaluated whether the HIV-1 gp120-induced arrest of $CD4^+$ T-cell migration resulted in the formation of VS with structures similar to those of the well-characterized IS. To address this question, we utilized the glass-supported planar bilayer system that has been extensively used for studying the IS (7, 22, 70). We previously demonstrated that proteins linked to the upper leaflet of the bilayers including GPI-anchored proteins and His_6-tagged soluble molecules captured through Ni^{2+}-chelating lipids are laterally mobile and, when fluorescently tagged, allow the visualization of receptor-ligand interactions in the interface with live cells (16, 59). The advantage of the planar substrate is that the system is optically ideal for the visualization of the interface in a single two-dimensional plane by wide-field, confocal, or total internal reflection illumination methods. The limitation is that the regulation of ligand lateral mobility and out-of-plane bending and fluctuations of biological membranes are not recapitulated by planar bilayers. We applied this model to the VS because prior cell-cell studies lacked the resolution to determine if SMACs are formed. Moreover, because the CD4-gp120 complex can potentially span up to ~28 nm, which is similar in size to an extended LFA-1 molecule, it is not obvious from structural models of CD4 and gp120 if they would be expected to segregate by size from LFA-1–ICAM-1 interactions (61).

Recombinant monomeric dual-tropic $HIV\text{-}1_{DH12}$ gp120 with a His_6 tag at its C terminus, which does not affect its CD4 and CKR binding abilities (9), was labeled with a green fluorescent dye, Alexa Fluor 488. The His_6-tagged gp120 was attached to the bilayers via Ni^{2+}-chelating NTA lipids, as previously described for His_6-tagged major histocompatibility complex class I molecules (59). We initially determined the binding capacity of the NTA lipids for gp120 by forming lipid bilayers on silica beads with liposomes containing different concentrations of Ni^{2+}-NTA lipids and then incubating them with 50 nM of Alexa Fluor 488-labeled His_6-gp120. The density of gp120 captured on the bilayer surface was measured by quantitative flow cytometry of the silica beads. Increasing densities of gp120 were observed on the bilayers as higher percentages of Ni^{2+}-NTA lipids were incorporated into the bilayers, and a maximal density of 600 molecules/μm^2 was achieved at 12.5% NTA (Fig. 3A), which was therefore used throughout the study. Subsequently, we determined the gp120 densities on 12.5% Ni^{2+}-NTA bilayers prepared with different concentrations of Alexa Fluor 488-gp120 (0 to 300 nM) (Fig. 3B). A linear relationship between gp120 concentrations used and the den-

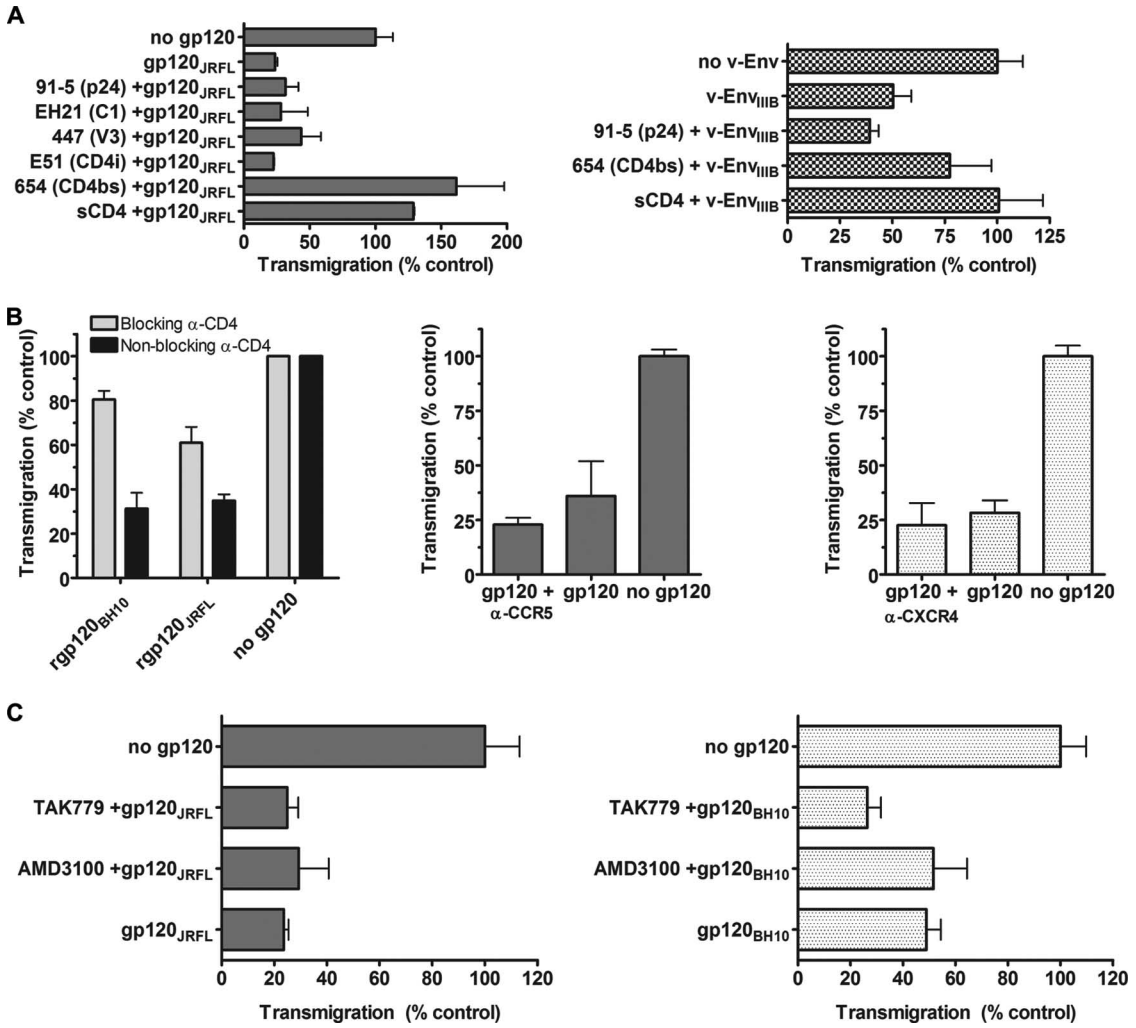

FIG. 2. HIV-1 envelope-induced transmigration arrest of human $CD4^+$ T cells is mediated by gp120-CD4 interaction. (A) The capacity of soluble CD4 (10 μg/ml) or MAbs (10 μg/ml) to the CD4bs (654), CD4i (E51), the V3 loop (447), or the C1 region in the N terminus of gp120 (EH21) to reverse the migration arrest induced by recombinant or native viral envelope ($gp120_{JRFL}$ or Env_{IIIB}) was evaluated. An anti-p24 MAb (91-5) was tested as an irrelevant control. (B) Anti-CD4 MAbs known to block or not block the gp120-CD4 interaction (RPA-T4 or OKT4, respectively), and MAbs to the CKRs CCR5 or CXCR4 (10 μg/ml) were tested for the capacity to restore the $CD4^+$ T-cell migration through filters coated with R5-tropic or X4-tropic gp120. (C) The effects of CCR5 or CXCR4 receptor antagonists (TAK779 or AMD3100 at 10 μM) on $CD4^+$ T-cell transmigration arrests mediated by the respective R5-tropic (JRFL) or X4-tropic (BH10) gp120 were also evaluated. Spontaneous migration in the presence of ICAM-1 alone ranged from 13% to 53% in the different experiments. For comparing the different reagents tested, the relative levels of transmigration were calculated, with spontaneous migration normalized to 100%. Representative data from one of two to three independent experiments are shown.

sities of gp120 loaded onto the bilayer surface, which ranged from 0 to 2,000 molecules per μm^2, was observed. This shows that fluorescently labeled gp120 can be successfully incorporated onto the bilayers at a wide range of densities, and hence, the planar bilayer system can be used as a model to study the interaction of the membrane-anchored HIV-1 envelope with live $CD4^+$ T cells. For comparison, gp120 expression on HIV-1-infected cells was estimated to be 640 molecules/cell based on the binding of fluorescein isothiocyanate-conjugated anti-gp120 MAb (654) to $CD4^+$ T cells infected with $HIV\text{-}1_{IIIB}$ (see Fig. S1 in the supplemental material), but most of the HIV-1 envelope glycoproteins are expressed in patches on infected cells (26, 51) and are also thought to cluster to lipid rafts (35, 38), and thus, the local density is expected to be much higher. On the surface of HIV-1 virions that are 100 nm in diameter, it is estimated that there are 8 to 14 trimeric envelope spikes per virion (71), which correspond to as much as 250 to 450 envelope spikes/μm^2. Therefore, we worked within this range. We used bilayers presenting anti-CD3 and ICAM-1 as a positive control for IS morphology.

Adhesion of $CD4^+$ T cells with bilayers presenting HIV-1 gp120 and ICAM-1. Activated $CD4^+$ T cells adhered to bilayers presenting gp120 and ICAM-1 (Fig. 4A), only ICAM-1 (Fig. 4B), or only gp120 (Fig. 4C), and images of randomly selected fields were acquired over 1 h. To allow the quantification of adhesion and cell motility, the same fields were acquired over 1 h (Fig. 4D and E). ICAM-1 and gp120 were presented at 250 molecules/μm^2 as indicated. The bright-field

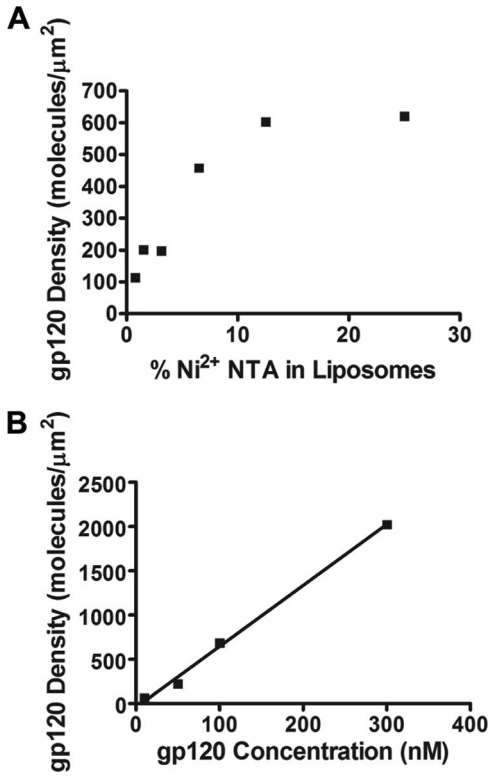

FIG. 3. Reconstitution of the planar bilayers with HIV-1 gp120. (A) Density of His_6-gp120 on silica beads coated with various concentrations of Ni^{2+}-chelating NTA liposomes. Silica beads were coated with liposome preparations containing 0.78% to 25% Ni^{2+}-NTA lipids and then treated with 50 nM Alexa Fluor 488-His_6-gp120. Quantitative flow cytometry was done with fluorescein calibration beads to calculate the density of gp120 in molecules/μm^2 on the surface of liposome-coated beads. (B) Density of gp120 on silica beads coated with different gp120 concentrations. Silica beads were coated with liposomes containing 12.5% Ni^{2+}-NTA and loaded with 10 to 300 nM Alexa Fluor 488-His_6-gp120. Quantitative flow cytometry was done as described above to determine the number of gp120 molecules per μm^2 on the bead surface. Representative data from one experiment are shown. This experiment was done routinely for each newly labeled gp120 batch used in the study.

image (Fig. 4A to C, top) shows all cells, the dark areas in the interference reflection microscopy (IRM) images (second panel) depict the close contact (<130 nm) that cells made with the bilayer, while the following third and the fourth panels show the fluorescence accumulation in the respective gp120 and ICAM-1 channels that represent receptor-ligand interactions. The activated $CD4^+$ T cells did not form any contacts in the absence of gp120 and ICAM-1 (data not shown). Bilayers presenting gp120 and ICAM-1 induced T cells to spread symmetrically, with large round contact areas. The accumulation of gp120 and ICAM-1 in the contact areas was segregated and took on the characteristic bull's-eye pattern of the IS, with a central cluster of gp120 accumulation surrounded by a ring of ICAM-1 accumulation. These cells coexisted with other cells that displayed various degrees of asymmetry, with elongated uropods (see below). Bilayers presenting ICAM-1 induced many polarized contact areas with an accumulation of ICAM-1 in an asymmetric lamella, similar to data reported in prior analyses (22, 57). Bilayers presenting gp120 induced smaller, generally round contacts with bright gp120 accumulation throughout the contact area.

We next evaluated the percent adhesion as the percentage of cells identified in bright-field imaging that had dark IRM signals of adherent cells, compared to the bright IRM signals of nonadherent cells. When the density of HIV-1 gp120 varied, we found that adhesion was dose dependent, with a threshold of around 25 molecules/μm^2 and a steady increase between 25 and 250 molecules/μm^2 (Fig. 4D, squares). The inclusion of ICAM-1 resulted in increased adhesion at a low gp120 density in the bilayer since ICAM-1 at 250 molecules/μm^2 was sufficient to mediate up to 80% adhesion, and adhesion was less than additive as gp120 was increased in the presence of a fixed density of ICAM-1 (Fig. 4D, triangles). We also measured the motility of the $CD4^+$ T cells as they interacted with the different bilayers. Bilayers presenting ICAM-1 alone induced continuous T-cell migration at an average speed of 5.7 μm/min, while bilayers presenting gp120 and ICAM-1 or gp120 induced migration at lower speeds of 1.8 and 1.6 μm/min, respectively (Fig. 4E). These data are consistent with the transmigration data presented above and demonstrate that the presence of HIV-1 gp120 retards spontaneous $CD4^+$ T-cell migration that occurs on ICAM-1-bearing surfaces.

Visualization of HIV-1 envelope-induced VS. We further compared the T-cell contacts with bilayers presenting gp120 and ICAM-1 with a control IS formed by the same T-cell preparations with bilayers containing anti-CD3 and ICAM-1. On bilayers containing anti-CD3 antibodies and ICAM-1, 90% of the $CD4^+$ T cells formed a mature IS, with anti-CD3 clustering into the cSMAC structure and ICAM-1 forming a symmetrical pSMAC ring (Fig. 5A, top two rows). Only a small percentage of the cells (10%) had asymmetrical pSMAC and were migratory (Fig. 5A, third row). By contrast, on the gp120 and ICAM-1 bilayers, three distinct patterns were observed at any one time during 1 h of observation (Fig. 5B to D). The percentages of the different morphologies observed on the bilayers with anti-CD3 and ICAM-1 and with gp120 and ICAM-1 are shown in Fig. 5G. Hence, one-fifth of the cells formed radial symmetrical structures similar in appearance to the IS; these contacts were characterized by a central gp120 accumulation surrounded by an intact ICAM-1 ring (Fig. 5B). These contacts were also positionally stable such that they meet a key criterion of a "synapse" and thus are a type of VS. One-third of cells had clearly defined areas of segregated gp120 and ICAM-1 but had off-center gp120 clusters and broken ICAM-1 rings and were slowly migratory (Fig. 5C). Thirteen percent of cells were elongated by 1 h due to a trailing uropod and long retraction fibers associated with bright gp120 and again had ICAM-1 accumulation at the leading edge with a very active lamellipodium (Fig. 5D). This morphology was not observed when T cells interacted with anti-CD3 antibody or cognate pMHC complexes, but the retraction fibers are reminiscence of structures called membrane nanotubes that were recently reported to connect migrating T cells and facilitate HIV-1 cell-to-cell transfer (60). These cells, like the proceeding category, were migratory and thus do not meet the definition of a synapse, so we do not count these as VS even though they have segregated gp120 interactions. The remaining one-third of adherent cells had ICAM-1 accumulation only with no gp120, similar to the cells contacting the bilayer with

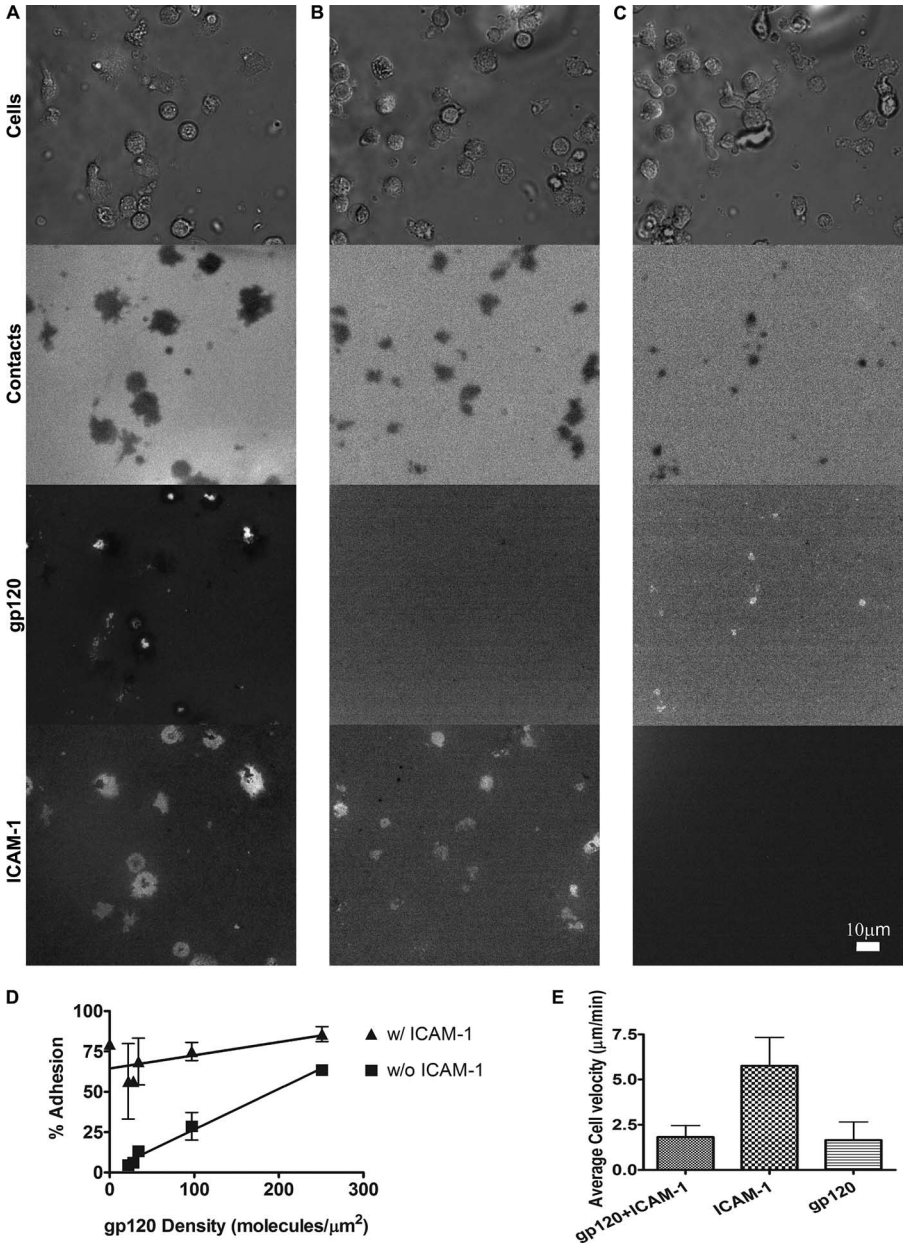

FIG. 4. $CD4^+$ T-cell interaction with lipid bilayers containing gp120 and ICAM-1, ICAM-1 alone, or gp120 alone. Activated human $CD4^+$ T cells were introduced into bilayers containing gp120 at 250 molecules/μm^2 and/or ICAM-1 at 250 molecules/μm^2. Images of randomly selected fields were acquired over 1 h. Representative whole-field images of activated $CD4^+$ T cells on gp120 and ICAM-1 (A), ICAM-1 (B), and gp120 (C) are shown. The top panels show the bright-field images of the cells, the second panels show the IRM images where the dark areas depict the bilayer surface contacted by the cells, and the third and fourth panels show gp120 and ICAM-1 fluorescence accumulation, respectively. (D) Percentages of cells adhering to the bilayers containing different densities of gp120. The numbers of cells contacting the bilayers were quantified based on the number of contacts observed in the IRM images over the total number of cells detected in the bright-field images. The graph shows the average values from three independent experiments. (E) Velocity of cells interacting with the bilayers. The speed of the individual cells migrating on the different bilayers was measured for 1 h. The graphs show the average cell velocities from three independent experiments. The numbers of cells analyzed were 206, 186, and 222 for gp120-and-ICAM-1, gp120, and ICAM-1 bilayers, respectively.

ICAM-1 alone (Fig. 5E); had gp120 accumulation only with no ICAM-1, similar to the cells on a bilayer with gp120 alone (Fig. 5F); or had no detectable ICAM-1 or gp120 accumulation. These distinct morphologies and the proportion of cells forming them were seen consistently with $CD4^+$ T cells from different donors. When activated $CD4^+$ T cells were introduced to bilayers containing anti-CD4 MAb and ICAM-1 (see Fig. S2 in the supplemental material), only 0.5% of the cells formed the symmetrical synapse (see Fig. S2A, top, in the supplemental material), while 27% of the cells remained migratory or were elongated with trailing uropods (see Fig. S2A, second and third panels, in the supplemental material). The remaining cells (45%) accumulated only anti-CD4 fluorescence similar to those of the cells observed on the gp120-alone bilayer (Fig. 5F

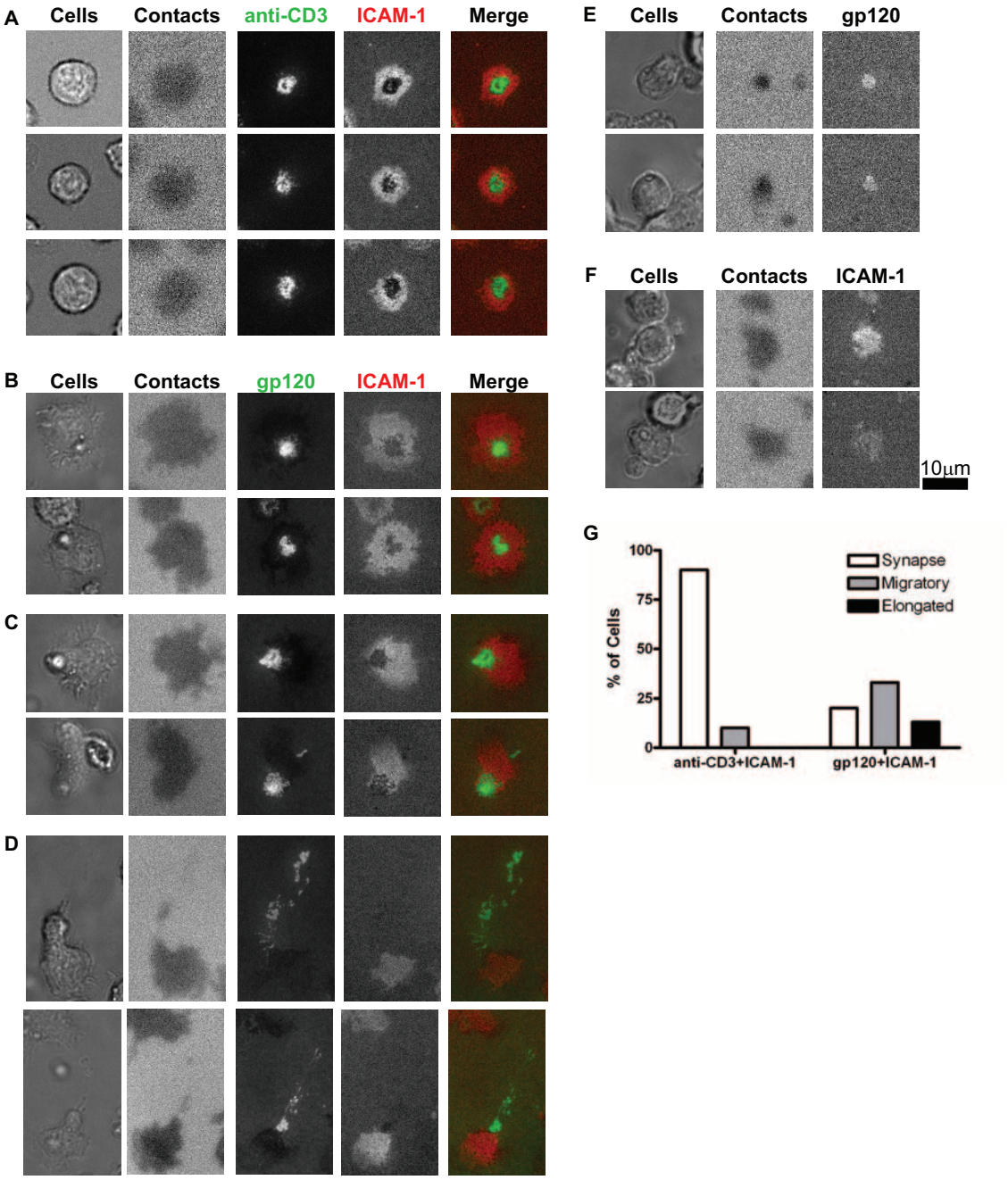

FIG. 5. HIV-1 gp120 induces assembly of a VS that shares a similar supramolecular organization with that of IS. Activated $CD4^+$ T cells were introduced to bilayers containing anti-CD3 and ICAM-1 (A), gp120 and ICAM-1 (B to D), ICAM-1 (E), or gp120 (F), and images were collected for 1 h. Representative images from one time point during the 1-h observation are shown. (G) The percentages of cells forming the different morphologies at any one time were calculated. The data shown are from one of at least three experiments performed independently with cells from different donors.

and see Fig. S2A, bottom, in the supplemental material). Hence, only HIV-1 gp120 efficiently induces changes in $CD4^+$ T-cell morphology, leading to the formation of a VS that shares supramolecular structures seen in the IS.

Observation of VS dissolution. Representative images for VS dynamics are shown in Fig. 6A (also see video image in Fig. S3 in the supplemental material). Two-thirds of activated $CD4^+$ T cells formed VS within 5 min after the cells were introduced to the bilayer and remained stable for an additional 15 to 20 min. At around 20 min, 95% of the T cells that formed the VS started to break symmetry of the ICAM-1 ring, and by 25 min, the T cells started to migrate through an asymmetrical contact that can further be developed into a highly elongated contact with gp120-positive retraction fibers as described above. Similarly, activated $CD4^+$ T cells on anti-CD3 and ICAM-1 bilayers (shown in Fig. 6B; also see video image in

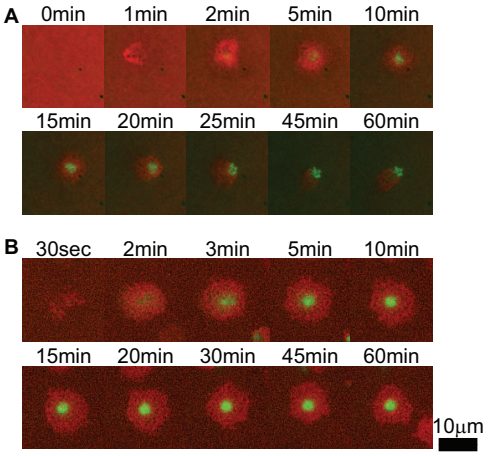

FIG. 6. Assembly and disassembly of the VS versus the IS. Activated $CD4^+$ T cells were introduced to bilayers containing gp120 and ICAM-1 (A) or anti-CD3 MAb and ICAM-1 (B), and the same fields were imaged for 1 h. The accumulation of fluorescence-labeled gp120 and anti-CD3 MAb is shown in green, while ICAM-1 accumulation is shown in red. In A, Cy5 fluorescence photobleached during the image acquisition. Images of one representative cell interacting with each bilayer at the indicated time points are shown; these images represent 95% of the cells forming a VS on the gp120-and-ICAM-1 bilayer and 90% of the cells on the anti-CD3-and-ICAM-1 bilayer.

Fig. S3 in the supplemental material) formed a mature IS within 5 min; however, 90% of the IS remained stable throughout the 1 h of imaging. Moreover, the cells on anti-CD3 and -ICAM-1 bilayers were more spread than the cells on gp120 and ICAM-1 bilayers. Therefore, while the VS and IS have a similar pattern, the gp120 cluster and ICAM-1 ring of the VS may not be truly analogous to cSMAC and pSMAC, respectively.

VS formation requires HIV-1 gp120 interaction with CD4 but not with the CKRs. To define the molecular interactions that drive VS formation, we applied the same panel of MAbs used in Fig. 2A for the control of migration to VS formation. The gp120 and ICAM-1 bilayers were treated with each MAb prior to cell injection, and the $CD4^+$ T cells were suspended in the buffer containing the MAb. After the cells were introduced to the bilayers, randomly selected fields were imaged for 1 h, and images were then quantified for the percentage of cells with gp120-positive contacts or ICAM-1-positive contacts and the areas of gp120 or ICAM-1 contacts. Blocking the gp120-CD4 interaction with the anti-CD4bs MAb drastically reduced the percentage of cells making gp120-positive contacts compared to the control ($P < 0.05$), while interfering gp120-CKR interaction with the anti-V3 MAb caused only a minor reduction, which was not statistically significant (Fig. 7A). The anti-CD4bs MAb also reduced the gp120-positive contact areas that the cells made, while, again, the anti-V3 MAb had no significant effect (Fig. 7C). Following T-cell activation, LFA-1 affinity increases 200-fold compared to its affinity on unstimulated T cells (42); therefore, neither of these blocking MAbs had any effect on $CD4^+$ T-cell interactions with ICAM-1 in terms of the number of cells with ICAM-1-positive contacts or the size of ICAM-1 contact areas (Fig. 7B and D). This indicates that for activated $CD4^+$ T cells, the interaction of gp120 and CD4

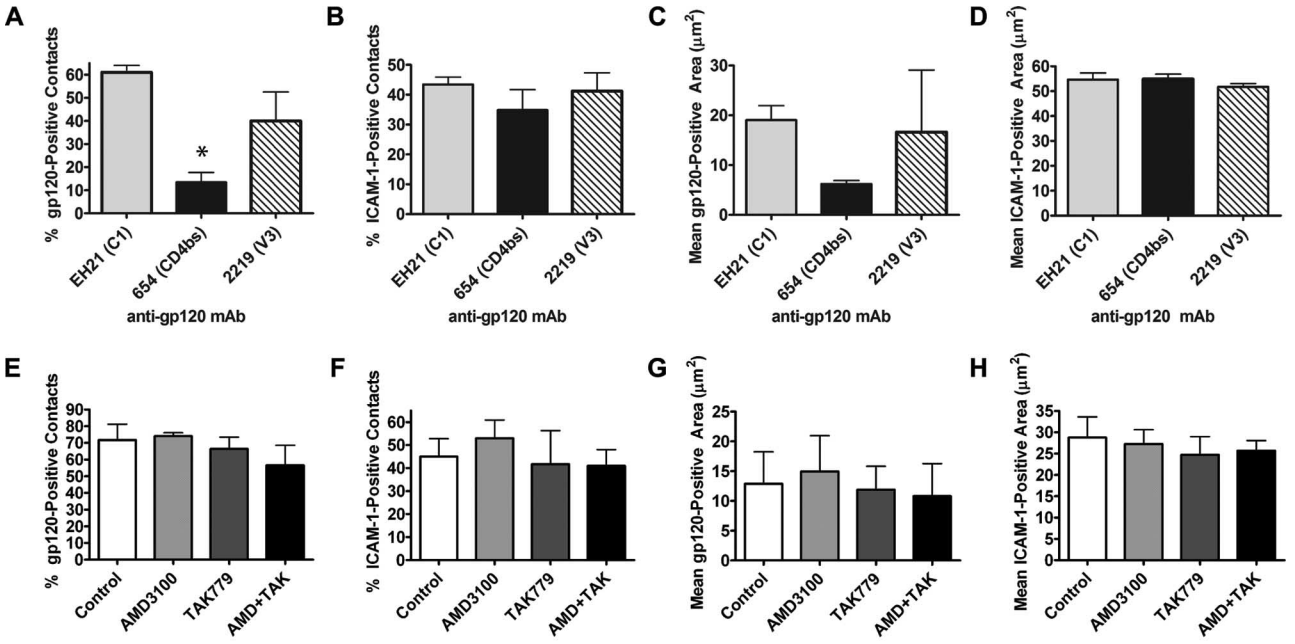

FIG. 7. VS formation requires gp120 interaction with CD4 but not with the CKR. Activated human $CD4^+$ T cells were introduced into gp120 and ICAM-1 bilayers in the presence of an anti-gp120 MAb that blocks the gp120-CD4 interaction (654), an anti-V3 MAb that interferes with the gp120 interaction with the CKR, or a control MAb against the N terminus of gp120 that does not affect gp120 binding to its receptors (EH21) (A to D) or in the presence of CKR antagonist AMD3100, TAK779, or both (E to H). The MAbs were used at 20 μg/ml, while AMD3100 and TAK779 were tested at 10 μM. The percentages of cells making gp120- and ICAM-1-positive contacts out of the total number of cells seen in the fields were calculated (A, B. E, and F). The areas of gp120-positive or ICAM-1-positive contact made by the cells on the bilayer were also measured (C, D, G, and H). Each graph shows averages from three independent experiments. *, $P < 0.05$ compared to MAb EH21-treated controls.

does not appear to deliver a signal for LFA-1 activation beyond the basal activation due to earlier in vitro activation with anti-CD3 and anti-CD28 MAb.

We further investigated the role of the gp120-CKR interaction in VS formation by testing the effects of a CXCR4 antagonist (AMD3100), a CCR5 antagonist (TAK779), or both. The antagonists were used at 10 μM each, as this concentration was found to completely block DH12 infection (30). These antagonists were added to $CD4^+$ T cells prior to their injection into the bilayer and kept throughout the assay. Images were acquired and analyzed as described above. Treatment with antagonists for CXCR4, CCR5, or both had no effect on the capacity of the $CD4^+$ T cells to form VS, as indicated by comparable numbers of cells forming gp120-positive and ICAM-1-positive contacts (Fig. 7E and G) and comparable sizes of the contact areas (Fig. 7F and H). These results show that VS formation requires gp120 binding to CD4 but does not involve a gp120-CKR interaction, and this is the same requirement for gp120-induced stop signals. In conclusion, this study demonstrates that the HIV-1 gp120 interaction with CD4 arrests the migration of activated human $CD4^+$ T cells, leading to the formation of the VS. The HIV-1 gp120-induced VS shares some common morphological features with the IS but is more transient and exhibits distinct dynamics.

DISCUSSION

This study provides evidence that surface-bound HIV-1 envelope gp120 induced a transient arrest of highly motile human $CD4^+$ T lymphocytes through the transient formation of a radially symmetrical VS. $CD4^+$ T cells, like other lymphocytes, are naturally migratory in vitro on ICAM-1-coated surfaces and in vivo as they actively crawl through lymphoid or nonlymphoid tissues (3, 14, 47). The migration arrest was triggered primarily by the gp120 interaction with the CD4 receptor on the cell surface without a significant involvement of the coreceptor CCR5 or CXCR4, suggesting that this is an early event that occurs soon after gp120 binding to CD4 prior to the subsequent processes needed for virus fusion and entry. The stopping was also readily reversible upon the SDF-1α engagement of the CXCR4 receptor on the cells. This is consistent with our findings that the CKR is not likely to be engaged in the gp120-mediated arrest of T-cell migration, and thus, SDF-1α can bind CXCR4 and attract the arrested T cells. Such transient stopping is in contrast to the stop signals induced by the TCR engagement, which is much more durable and resistant to chemoattraction by the SDF-1α chemokine gradient, thus indicating that unique signals and activation patterns are triggered in $CD4^+$ T cells upon binding with HIV-1 gp120. HIV-1 gp120 has also been shown to act like a chemoattractant and influence T-cell migration in CD4-dependent and CD4-independent manners. However, the stopping effect reported here is distinct from the chemotactic capacity of cell-free HIV-1 or simian immunodeficiency virus and soluble virus envelope proteins to attract $CD4^+$ T cells or $CD8^+$ T cells (4, 31, 32). It also differs from the CXCR4-mediated repelling effect of high concentrations of soluble HIV-1 gp120 on $CD8^+$ T cells (4).

Importantly, we demonstrate that the stopping was associated with the formation of the VS in which gp120, upon interacting with $CD4^+$ T cells, accumulated in the center of the VS and segregated from the adhesion molecule ICAM-1, which formed a ring structure around the gp120 central cluster. The VS morphology observed in our planar bilayer model is consistent with previously published data from the cell-cell conjugate system where HIV-1 or human T-cell lymphotropic virus type 1 *env* and *gag* indeed form a cap, along with ICAM-1 and LFA-1, on the VS interface between an infected cell and a target $CD4^+$ T cell, and the actin anchor protein talin, which is associated with LFA-1, is found frequently in partial ring-like clusters (29, 35). Nevertheless, images obtained from cell-cell conjugates provided only the side view of the synapse, and the resolution did not permit a clear identification of the supramolecular organization, as can be observed in the planar bilayer model, especially for molecules that can be present in both HIV-1-infected cells and target cells such as CD4 and LFA-1. Of note, other $CD4^+$ cells like macrophages (G. Vasiliver-Shamis et al., unpublished results) and DC-$SIGN^+$ cells can induce VS formation with noninfected $CD4^+$ T cells and may disseminate HIV-1 through common mechanisms such as those described for the T-cell–T-cell VS (24, 44).

VS formation was induced specifically upon the HIV-1 gp120 interaction with CD4 and could not be mimicked fully by antibodies to CD4, even though both gp120 and anti-CD4 antibodies were able to arrest $CD4^+$ T-cell migration transiently. These results suggest that unique downstream signals are triggered upon the HIV-1 gp120 interaction with CD4 to generate the VS. It is also important that, like activated $CD4^+$ T cells studied here, naïve $CD4^+$ T cells could form similar VS structures (Vasiliver-Shamis et al., unpublished), suggesting that prior TCR-mediated activation is not necessary for VS assembly. However, the LFA-1–ICAM-1 interaction that creates the peripheral adhesion ring requires LFA-1 activation. On activated T cells, LFA-1 is found in its active conformation (42), but on unstimulated (naïve and memory) cells, LFA-1 needs to convert from a closed conformation to an extended, active conformation. Whether the gp120-CD4 interaction induces LFA-1 activation to lead to VS formation remains unclear and is under investigation. However, it was recently shown that the gp120-α4β7 interaction in resting memory cells can induce LFA-1 activation (1).

The symmetrical adhesion ring has been shown to be essential for stopping migratory T lymphocytes in the absence of antigen as well as during IS formation upon TCR engagement of specific pMHC complexes and may function similarly in the VS. In the absence of gp120, no ICAM-1 ring was ever observed. Similarly, when the gp120-CD4 interaction was blocked with MAbs, the ICAM-1 ring was also not formed, indicating that adhesion ring formation is triggered by gp120 binding to the $CD4^+$ T cells. Nevertheless, the arrest of migration by HIV-1 gp120 was short-lived; after 15 to 20 min, the ICAM-1 ring symmetry broke, and the cells became migratory and did not appear to reform a new VS during the 1-h observation period. In contrast, a mature IS can be maintained for over 1 h. A recent report by Sims et al. also showed that naïve T cells forming a mature IS could break the symmetry of the ICAM-1 ring and migrated, but they reformed a new synapse at a different site (56). What prevents the $CD4^+$ T cells that have formed and broke VS to assemble a new VS is unknown. It is possible that after forming the VS, these cells downregulate

their CD4 surface expression (2, 46, 67), or alternatively, downstream signals that prevent the subsequent migration arrest, at least for the duration of the experiment, i.e., 1 h, are triggered. Wiscott-Aldrich syndrome protein (WASp)-deficient cells displayed a similar behavior, suggesting that the regulation of Cdc42 and WASp could be involved (56, 63). Regardless of the mechanisms, one may speculate that the $CD4^+$ T cells breaking off the VS and taking the virus would eventually become infected and express the HIV-1 envelope gp120 on the cell surface, and these cells would in turn arrest the migration of other susceptible $CD4^+$ target cells to form a VS and continue the spread of the virus.

While a proportion of the $CD4^+$ T cells transiently stopped migrating on the bilayers with gp120 and ICAM-1, some other cells did not completely stop and remained migratory. However, on average, the migration rates of all cells were significantly reduced compared to those observed on bilayers with ICAM-1 alone. If the scenario here reflects the migration patterns of target $CD4^+$ T cells following VS formation and virus acquisition from infected cells, this may constitute a highly effective mechanism for HIV-1 spread in lymphoid tissues. We propose that HIV-1 gp120-mediated transient stopping or slowing down of highly motile $CD4^+$ T cells may allow virus transfer and acquisition but may not be sufficiently sustained for virus envelope-mediated fusion, which requires the recruitment of the appropriate CKRs and is relatively slow, with a lag phase of ~30 min and a half-life of at least 1 h (20). Hence, the quick detachment of target $CD4^+$ T cells from infected cells after virus acquisition may prevent cell-cell fusion, which would terminate the virus life cycle while enhancing the rate of virus spread to new target cells and to more distant sites in tissues. This idea is consistent with our data showing that both gp120-induced VS formation and migration arrest are triggered transiently, soon after gp120 interacts with CD4, without the involvement of the CKR. A recent report by Chen et al. also demonstrated that the efficient cell-to-cell transfer of R5-tropic HIV-1 via the VS was dependent on the gp120-CD4 interaction and did not require CCR5 to be expressed on the target cell (8). Furthermore, the fact that the VS is not as stable as the IS implies that the VS may not induce as complete a T-cell activation as the IS (22). Ongoing studies in our laboratory are examining these possibilities by evaluating the signaling events triggered by the VS compared to those triggered by the IS. However, previously reported data have shown that gp120 induces signaling via CD4, the chemokine receptor CCR5, or the $\alpha 4\beta 7$ integrin and can trigger calcium mobilization, a trademark readout for T-cell activation (1, 10, 11, 40, 45, 69). Additionally, CD4 engagement by an anti-CD4 MAb was shown to be sufficient for Lck activation (28), although the subsequent signaling events and how they differ from those triggered by gp120 are unclear at this point. HIV-1 replication within $CD4^+$ T cells is tightly linked to their activation state but requires a balance between a state of activation that relieves the blocks of early postreplication events and hyperactivation that leads to host cell death (43, 62). HIV-1 potentially exploits VS not only for facilitating its dissemination within the host but also for inducing T-cell activation to a level that is sufficient to support its replication without incurring premature cell death.

In conclusion, we demonstrated that HIV-1 envelope gp120 induced the transient arrest of naturally motile $CD4^+$ T cells and that the stopping was associated with the formation of the VS, which displayed supramolecular clusters, as observed in the IS. A better understanding of the molecular details and biological functions of the VS may lead to the development of novel intervention strategies that block this efficient and concealed mode used by HIV-1 to spread from cell to cell in infected hosts.

ACKNOWLEDGMENTS

This paper is dedicated to the memory of our colleague and friend Toby Starr.

We thank Diana Virland for assistance with flow cytometry.

This work was supported in part by NIH grants AI43542 (M.L.D.), AI44931 (M.L.D.), AI-060503 (M.W.C.), and AI071815 (C.E.H.) as well as a merit review award and the Research Enhancement Award Program of the U.S. Department of Veterans Affairs, New York University Center for AIDS Research (AI-27742), Case Western Reserve University Center for AIDS Research (AI-36219), and the Training Program in TB and HIV Prevention and Treatment (D43 TWO1409).

REFERENCES

1. **Arthos, J., C. Cicala, E. Martinelli, K. Macleod, D. Van Ryk, D. Wei, Z. Xiao, T. D. Veenstra, T. P. Conrad, R. A. Lempicki, S. McLaughlin, M. Pascuccio, R. Gopaul, J. McNally, C. C. Cruz, N. Censoplano, E. Chung, K. N. Reitano, S. Kottilil, D. J. Goode, and A. S. Fauci.** 2008. HIV-1 envelope protein binds to and signals through integrin alpha4beta7, the gut mucosal homing receptor for peripheral T cells. Nat. Immunol. **9:**301–309.
2. **Benson, R. E., A. Sanfridson, J. S. Ottinger, C. Doyle, and B. R. Cullen.** 1993. Downregulation of cell-surface CD4 expression by simian immunodeficiency virus Nef prevents viral super infection. J. Exp. Med. **177:**1561–1566.
3. **Bradl, M., J. Bauer, A. Flugel, H. Wekerle, and H. Lassmann.** 2005. Complementary contribution of CD4 and CD8 T lymphocytes to T-cell infiltration of the intact and the degenerative spinal cord. Am. J. Pathol. **166:**1441–1450.
4. **Brainard, D. M., W. G. Tharp, E. Granado, N. Miller, A. K. Trocha, X. H. Ren, B. Conrad, E. F. Terwilliger, R. Wyatt, B. D. Walker, and M. C. Poznansky.** 2004. Migration of antigen-specific T cells away from CXCR4-binding human immunodeficiency virus type 1 gp120. J. Virol. **78:**5184–5193.
5. **Bromley, S. K., D. A. Peterson, M. D. Gunn, and M. L. Dustin.** 2000. Cutting edge: hierarchy of chemokine receptor and TCR signals regulating T cell migration and proliferation. J. Immunol. **165:**15–19.
6. **Bunnell, S. C., D. I. Hong, J. R. Kardon, T. Yamazaki, C. J. McGlade, V. A. Barr, and L. E. Samelson.** 2002. T cell receptor ligation induces the formation of dynamically regulated signaling assemblies. J. Cell Biol. **158:**1263–1275.
7. **Carrasco, Y. R., S. J. Fleire, T. Cameron, M. L. Dustin, and F. D. Batista.** 2004. LFA-1/ICAM-1 interaction lowers the threshold of B cell activation by facilitating B cell adhesion and synapse formation. Immunity **20:**589–599.
8. **Chen, P., W. Hubner, M. A. Spinelli, and B. K. Chen.** 2007. Predominant mode of human immunodeficiency virus transfer between T cells is mediated by sustained Env-dependent neutralization-resistant virological synapses. J. Virol. **81:**12582–12595.
9. **Cho, M. W., Y. B. Kim, M. K. Lee, K. C. Gupta, W. Ross, R. Plishka, A. Buckler-White, T. Igarashi, T. Theodore, R. Byrum, C. Kemp, D. C. Montefiori, and M. A. Martin.** 2001. Polyvalent envelope glycoprotein vaccine elicits a broader neutralizing antibody response but is unable to provide sterilizing protection against heterologous simian/human immunodeficiency virus infection in pigtailed macaques. J. Virol. **75:**2224–2234.
10. **Cicala, C., J. Arthos, M. Ruiz, M. Vaccarezza, A. Rubbert, A. Riva, K. Wildt, O. Cohen, and A. S. Fauci.** 1999. Induction of phosphorylation and intracellular association of CC chemokine receptor 5 and focal adhesion kinase in primary human CD4+ T cells by macrophage-tropic HIV envelope. J. Immunol. **163:**420–426.
11. **Davis, C. B., I. Dikic, D. Unutmaz, C. M. Hill, J. Arthos, M. A. Siani, D. A. Thompson, J. Schlessinger, and D. R. Littman.** 1997. Signal transduction due to HIV-1 envelope interactions with chemokine receptors CXCR4 or CCR5. J. Exp. Med. **186:**1793–1798.
12. **Dimitrov, D. S., R. L. Willey, H. Sato, L. J. Chang, R. Blumenthal, and M. A. Martin.** 1993. Quantitation of human immunodeficiency virus type 1 infection kinetics. J. Virol. **67:**2182–2190.
13. **Donnadieu, E., G. Bismuth, and A. Trautmann.** 1994. Antigen recognition by helper T cells elicits a sequence of distinct changes of their shape and intracellular calcium. Curr. Biol. **4:**584–595.
14. **Dustin, M. L., S. K. Bromley, Z. Kan, D. A. Peterson, and E. R. Unanue.** 1997. Antigen receptor engagement delivers a stop signal to migrating T lymphocytes. Proc. Natl. Acad. Sci. USA **94:**3909–3913.

15. **Dustin, M. L., and D. R. Colman.** 2002. Neural and immunological synaptic relations. Science **298:**785–789.
16. **Dustin, M. L., J. M. Miller, S. Ranganath, D. A. Vignali, N. J. Viner, C. A. Nelson, and E. R. Unanue.** 1996. TCR-mediated adhesion of T cell hybridomas to planar bilayers containing purified MHC class II/peptide complexes and receptor shedding during detachment. J. Immunol. **157:**2014–2021.
17. **Dustin, M. L., M. W. Olszowy, A. D. Holdorf, J. Li, S. Bromley, N. Desai, P. Widder, F. Rosenberger, P. A. van der Merwe, P. M. Allen, and A. S. Shaw.** 1998. A novel adaptor protein orchestrates receptor patterning and cytoskeletal polarity in T-cell contacts. Cell **94:**667–677.
18. **Dustin, M. L., and A. S. Shaw.** 1999. Costimulation: building an immunological synapse. Science **283:**649–650.
19. **Frank, I., H. Stoiber, S. Godar, H. Stockinger, F. Steindl, H. W. Katinger, and M. P. Dierich.** 1996. Acquisition of host cell-surface-derived molecules by HIV-1. AIDS **10:**1611–1620.
20. **Gallo, S. A., J. D. Reeves, H. Garg, B. Foley, R. W. Doms, and R. Blumenthal.** 2006. Kinetic studies of HIV-1 and HIV-2 envelope glycoprotein-mediated fusion. Retrovirology **3:**90.
21. **Garrido, M., A. Mozos, A. Martinez, F. Garcia, A. Serafin, V. Morente, M. Caballero, C. Gil, E. Fumero, J. M. Miro, N. Climent, J. M. Gatell, and L. Alos.** 2007. HIV-1 upregulates intercellular adhesion molecule-1 gene expression in lymphoid tissue of patients with chronic HIV-1 infection. J. Acquir. Immune Defic. Syndr. **46:**268–274.
22. **Grakoui, A., S. K. Bromley, C. Sumen, M. M. Davis, A. S. Shaw, P. M. Allen, and M. L. Dustin.** 1999. The immunological synapse: a molecular machine controlling T cell activation. Science **285:**221–227.
23. **Groot, F., T. W. Kuijpers, B. Berkhout, and E. C. de Jong.** 2006. Dendritic cell-mediated HIV-1 transmission to T cells of LAD-1 patients is impaired due to the defect in LFA-1. Retrovirology **3:**75.
24. **Groot, F., S. Welsch, and Q. J. Sattentau.** 2008. Efficient HIV-1 transmission from macrophages to T cells across transient virological synapses. Blood **111:**4660–4663.
25. **Haynes, B. F., J. Fleming, E. W. St. Clair, H. Katinger, G. Stiegler, R. Kunert, J. Robinson, R. M. Scearce, K. Plonk, H. F. Staats, T. L. Ortel, H. X. Liao, and S. M. Alam.** 2005. Cardiolipin polyspecific autoreactivity in two broadly neutralizing HIV-1 antibodies. Science **308:**1906–1908.
26. **Hermida-Matsumoto, L., and M. D. Resh.** 2000. Localization of human immunodeficiency virus type 1 Gag and Env at the plasma membrane by confocal imaging. J. Virol. **74:**8670–8679.
27. **Hioe, C. E., P. C. Chien, Jr., C. Lu, T. A. Springer, X. H. Wang, J. Bandres, and M. Tuen.** 2001. LFA-1 expression on target cells promotes human immunodeficiency virus type 1 infection and transmission. J. Virol. **75:**1077–1082.
28. **Holdorf, A. D., K. H. Lee, W. R. Burack, P. M. Allen, and A. S. Shaw.** 2002. Regulation of Lck activity by CD4 and CD28 in the immunological synapse. Nat. Immunol. **3:**259–264.
29. **Igakura, T., J. C. Stinchcombe, P. K. Goon, G. P. Taylor, J. N. Weber, G. M. Griffiths, Y. Tanaka, M. Osame, and C. R. Bangham.** 2003. Spread of HTLV-I between lymphocytes by virus-induced polarization of the cytoskeleton. Science **299:**1713–1716.
30. **Igarashi, T., Y. Endo, Y. Nishimura, C. Buckler, R. Sadjadpour, O. K. Donau, M. J. Dumaurier, R. J. Plishka, A. Buckler-White, and M. A. Martin.** 2003. Early control of highly pathogenic simian immunodeficiency virus/human immunodeficiency virus chimeric virus infections in rhesus monkeys usually results in long-lasting asymptomatic clinical outcomes. J. Virol. **77:**10829–10840.
31. **Iyengar, S., D. H. Schwartz, J. E. Clements, and J. E. Hildreth.** 2000. CD4-independent, CCR5-dependent simian immunodeficiency virus infection and chemotaxis of human cells. J. Virol. **74:**6720–6724.
32. **Iyengar, S., D. H. Schwartz, and J. E. Hildreth.** 1999. T cell-tropic HIV gp120 mediates CD4 and CD8 cell chemotaxis through CXCR4 independent of CD4: implications for HIV pathogenesis. J. Immunol. **162:**6263–6267.
33. **Izzard, C. S., and L. R. Lochner.** 1976. Cell-to-substrate contacts in living fibroblasts: an interference reflexion study with an evaluation of the technique. J. Cell Sci. **21:**129–159.
34. **Johnston, S. C., M. L. Dustin, M. L. Hibbs, and T. A. Springer.** 1990. On the species specificity of the interaction of LFA-1 with intercellular adhesion molecules. J. Immunol. **145:**1181–1187.
35. **Jolly, C., K. Kashefi, M. Hollinshead, and Q. J. Sattentau.** 2004. HIV-1 cell to cell transfer across an Env-induced, actin-dependent synapse. J. Exp. Med. **199:**283–293.
36. **Jolly, C., I. Mitar, and Q. J. Sattentau.** 2007. Adhesion molecule interactions facilitate human immunodeficiency virus type 1-induced virological synapse formation between T cells. J. Virol. **81:**13916–13921.
37. **Jolly, C., I. Mitar, and Q. J. Sattentau.** 2007. Requirement for an intact T-cell actin and tubulin cytoskeleton for efficient assembly and spread of human immunodeficiency virus type 1. J. Virol. **81:**5547–5560.
38. **Jolly, C., and Q. J. Sattentau.** 2005. Human immunodeficiency virus type 1 virological synapse formation in T cells requires lipid raft integrity. J. Virol. **79:**12088–12094.
39. **Jolly, C., and Q. J. Sattentau.** 2004. Retroviral spread by induction of virological synapses. Traffic **5:**643–650.
40. **Juszczak, R. J., H. Turchin, A. Truneh, J. Culp, and S. Kassis.** 1991. Effect of human immunodeficiency virus gp120 glycoprotein on the association of the protein tyrosine kinase p56lck with CD4 in human T lymphocytes. J. Biol. Chem. **266:**11176–11183.
41. **Labrosse, B., A. Brelot, N. Heveker, N. Sol, D. Schols, E. De Clercq, and M. Alizon.** 1998. Determinants for sensitivity of human immunodeficiency virus coreceptor CXCR4 to the bicyclam AMD3100. J. Virol. **72:**6381–6388.
42. **Lollo, B. A., K. W. Chan, E. M. Hanson, V. T. Moy, and A. A. Brian.** 1993. Direct evidence for two affinity states for lymphocyte function-associated antigen 1 on activated T cells. J. Biol. Chem. **268:**21693–21700.
43. **Matarrese, P., and W. Malorni.** 2005. Human immunodeficiency virus (HIV)-1 proteins and cytoskeleton: partners in viral life and host cell death. Cell Death Differ. **12**(Suppl. 1)**:**932–941.
44. **McDonald, D., L. Wu, S. M. Bohks, V. N. KewalRamani, D. Unutmaz, and T. J. Hope.** 2003. Recruitment of HIV and its receptors to dendritic cell-T cell junctions. Science **300:**1295–1297.
45. **Melar, M., D. E. Ott, and T. J. Hope.** 2007. Physiological levels of virion-associated human immunodeficiency virus type 1 envelope induce coreceptor-dependent calcium flux. J. Virol. **81:**1773–1785.
46. **Michel, N., K. Ganter, S. Venzke, J. Bitzegeio, O. T. Fackler, and O. T. Keppler.** 2006. The Nef protein of human immunodeficiency virus is a broad-spectrum modulator of chemokine receptor cell surface levels that acts independently of classical motifs for receptor endocytosis and Galphai signaling. Mol. Biol. Cell **17:**3578–3590.
47. **Miller, M. J., S. H. Wei, I. Parker, and M. D. Cahalan.** 2002. Two-photon imaging of lymphocyte motility and antigen response in intact lymph node. Science **296:**1869–1873.
48. **Monks, C. R., B. A. Freiberg, H. Kupfer, N. Sciaky, and A. Kupfer.** 1998. Three-dimensional segregation of supramolecular activation clusters in T cells. Nature **395:**82–86.
49. **Negulescu, P. A., T. B. Krasieva, A. Khan, H. H. Kerschbaum, and M. D. Cahalan.** 1996. Polarity of T cell shape, motility, and sensitivity to antigen. Immunity **4:**421–430.
50. **Nguyen, K., N. R. Sylvain, and S. C. Bunnell.** 2008. T cell costimulation via the integrin VLA-4 inhibits the actin-dependent centralization of signaling microclusters containing the adaptor SLP-76. Immunity **28:**810–821.
51. **Nydegger, S., S. Khurana, D. N. Krementsov, M. Foti, and M. Thali.** 2006. Mapping of tetraspanin-enriched microdomains that can function as gateways for HIV-1. J. Cell Biol. **173:**795–807.
52. **Paquette, J. S., J. F. Fortin, L. Blanchard, and M. J. Tremblay.** 1998. Level of ICAM-1 surface expression on virus producer cells influences both the amount of virion-bound host ICAM-1 and human immunodeficiency virus type 1 infectivity. J. Virol. **72:**9329–9336.
53. **Pearce-Pratt, R., D. Malamud, and D. M. Phillips.** 1994. Role of the cytoskeleton in cell-to-cell transmission of human immunodeficiency virus. J. Virol. **68:**2898–2905.
54. **Peters, P. J., J. Bhattacharya, S. Hibbitts, M. T. Dittmar, G. Simmons, J. Bell, P. Simmonds, and P. R. Clapham.** 2004. Biological analysis of human immunodeficiency virus type 1 R5 envelopes amplified from brain and lymph node tissues of AIDS patients with neuropathology reveals two distinct tropism phenotypes and identifies envelopes in the brain that confer an enhanced tropism and fusigenicity for macrophages. J. Virol. **78:**6915–6926.
55. **Schmoranzer, J., M. Goulian, D. Axelrod, and S. M. Simon.** 2000. Imaging constitutive exocytosis with total internal reflection fluorescence microscopy. J. Cell Biol. **149:**23–32.
56. **Sims, T. N., T. J. Soos, H. S. Xenias, B. Dubin-Thaler, J. M. Hofman, J. C. Waite, T. O. Cameron, V. K. Thomas, R. Varma, C. H. Wiggins, M. P. Sheetz, D. R. Littman, and M. L. Dustin.** 2007. Opposing effects of PKCtheta and WASp on symmetry breaking and relocation of the immunological synapse. Cell **129:**773–785.
57. **Smith, A., Y. R. Carrasco, P. Stanley, N. Kieffer, F. D. Batista, and N. Hogg.** 2005. A talin-dependent LFA-1 focal zone is formed by rapidly migrating T lymphocytes. J. Cell Biol. **170:**141–151.
58. **Sol-Foulon, N., M. Sourisseau, F. Porrot, M. I. Thoulouze, C. Trouillet, C. Nobile, F. Blanchet, V. di Bartolo, N. Noraz, N. Taylor, A. Alcover, C. Hivroz, and O. Schwartz.** 2007. ZAP-70 kinase regulates HIV cell-to-cell spread and virological synapse formation. EMBO J. **26:**516–526.
59. **Somersalo, K., N. Anikeeva, T. N. Sims, V. K. Thomas, R. K. Strong, T. Spies, T. Lebedeva, Y. Sykulev, and M. L. Dustin.** 2004. Cytotoxic T lymphocytes form an antigen-independent ring junction. J. Clin. Investig. **113:**49–57.
60. **Sowinski, S., C. Jolly, O. Berninghausen, M. A. Purbhoo, A. Chauveau, K. Kohler, S. Oddos, P. Eissmann, F. M. Brodsky, C. Hopkins, B. Onfelt, Q. Sattentau, and D. M. Davis.** 2008. Membrane nanotubes physically connect T cells over long distances presenting a novel route for HIV-1 transmission. Nat. Cell Biol. **10:**211–219.
61. **Springer, T. A.** 1990. Adhesion receptors of the immune system. Nature **346:**425–434.
62. **Stevenson, M.** 2003. HIV-1 pathogenesis. Nat. Med. **9:**853–860.
63. **Stowers, L., D. Yelon, L. J. Berg, and J. Chant.** 1995. Regulation of the polarization of T cells toward antigen-presenting cells by Ras-related GTPase CDC42. Proc. Natl. Acad. Sci. USA **92:**5027–5031.

64. **Tardif, M. R., and M. J. Tremblay.** 2005. LFA-1 is a key determinant for preferential infection of memory CD4+ T cells by human immunodeficiency virus type 1. J. Virol. **79:**13714–13724.
65. **Tardif, M. R., and M. J. Tremblay.** 2003. Presence of host ICAM-1 in human immunodeficiency virus type 1 virions increases productive infection of CD4+ T lymphocytes by favoring cytosolic delivery of viral material. J. Virol. **77:**12299–12309.
66. **Tardif, M. R., and M. J. Tremblay.** 2005. Regulation of LFA-1 activity through cytoskeleton remodeling and signaling components modulates the efficiency of HIV type-1 entry in activated CD4+ T lymphocytes. J. Immunol. **175:**926–935.
67. **Venzke, S., N. Michel, I. Allespach, O. T. Fackler, and O. T. Keppler.** 2006. Expression of Nef downregulates CXCR4, the major coreceptor of human immunodeficiency virus, from the surfaces of target cells and thereby enhances resistance to superinfection. J. Virol. **80:**11141–11152.
68. **Visciano, M. L., M. Tuen, M. K. Gorny, and C. E. Hioe.** 2008. In vivo alteration of humoral responses to HIV-1 envelope glycoprotein gp120 by antibodies to the CD4-binding site of gp120. Virology **372:**409–420.
69. **Weissman, D., R. L. Rabin, J. Arthos, A. Rubbert, M. Dybul, R. Swofford, S. Venkatesan, J. M. Farber, and A. S. Fauci.** 1997. Macrophage-tropic HIV and SIV envelope proteins induce a signal through the CCR5 chemokine receptor. Nature **389:**981–985.
70. **Yokosuka, T., K. Sakata-Sogawa, W. Kobayashi, M. Hiroshima, A. Hashimoto-Tane, M. Tokunaga, M. L. Dustin, and T. Saito.** 2005. Newly generated T cell receptor microclusters initiate and sustain T cell activation by recruitment of Zap70 and SLP-76. Nat. Immunol. **6:**1253–1262.
71. **Zhu, P., J. Liu, J. Bess, Jr., E. Chertova, J. D. Lifson, H. Grise, G. A. Ofek, K. A. Taylor, and K. H. Roux.** 2006. Distribution and three-dimensional structure of AIDS virus envelope spikes. Nature **441:**847–852.
72. **Zolla-Pazner, S.** 2004. Identifying epitopes of HIV-1 that induce protective antibodies. Nat. Rev. Immunol. **4:**199–210.